UNIVERSITY OF TARTU
Faculty of Science and Technology
Institute of Physics

Kärt Soieva

THE COOLING PROCESS OF BROWN DWARFS IN HORNDESKI THEORY OF GRAVITY

Bachelor's thesis (6 ECTS)
Physics, Chemistry and Material Science

Supervisor:
Aneta Wojnar, PhD

Tartu 2022

The cooling process of brown dwarfs in Horndeski theory of gravity

The main result of the work showcased in this thesis is an analytical model for the evolution of a brown dwarf star in Horndeski theory of gravity. In comparison to the main sequence stars, no energy is produced in the brown dwarf's interior, therefore they gradually lose stored heat and cool down with time. We investigate how the cooling model of such substellar objects in modified theory of gravity differs from the one in Newtonian gravity. The theory under study is the scalar-tensor theory of gravity, which is one of the most popular alternatives to the general theory of relativity. Firstly, analytical formulae characterising the cooling process are derived. Secondly, the equations are numerically solved and results plotted. Lastly, the differences in the cooling models in Newtonian and Horndeski gravity are discussed.

Keywords: brown dwarf, cooling model, modified gravity, Horndeski
CERCS: P190 — Mathematical and general theoretical physics, classical mechanics, quantum mechanics, relativity, gravitation, statistical physics, thermodynamics

Pruunide kääbuste jahtumisprotsess Horndeski gravitatsiooniteoorias

Töö tulemusena valmib analüütiline mudel, mis kirjeldab pruunide kääbuste jahtumisprotsessi Horndeski gravitatsiooniteoorias. Pruunid kääbused on väiksemad kui peajada tähed, mistõttu ei toodeta nende sisemuses energiat ning ajapikku jahtuvad nad maha. Meie uurime, kuidas mõjutab Horndeski gravitatsiooniteooria sisse toomine jahtumist kirjeldavat mudelit võrreldes Newtoni teooriaga. Horndeski teooria on üks mitmest alternatiivist Einsteini üldrelatiivsusteooriale. Esmalt, tuletame analüütilised valemid, mis kirjeldavad pruunide kääbuste jahtumist. Seejärel, lahendame need võrrandid numbriliselt ja joonistame tulemustest graafikud. Lõpuks analüüsime, millised on erinevused jahtumismudelis Newtoni ja Horndeski gravitatsiooniteooriates.

Märksõnad: pruun kääbus, jahtumisprotsess, modifitseeritud gravitatsiooniteooria, Horndeski
CERCS: P190 — Matemaatiline ja üldine teoreetiline füüsika, klassikaline mehaanika, kvantmehaanika, relatiivsus, gravitatsioon, statistiline füüsika, termodünaamika

Contents

Introduction

The existence of brown dwarf stars or rather a class between planets and main-sequence stars was firstly theorised in 1962 by S. S. Kumar [1]. However, they were confirmed by observations in 1995 [2]. Since then we have been receiving more information about those objects with many space telescopes recently launched into the orbit. We are living in an exciting era to study brown dwarfs owing to the fact that many future missions have already been planned utilising advanced technology, which will now be used to investigate brown dwarfs. These missions are also included in European Space Agency's 'Cosmic Vision 2015-2025', which is the current long-term plan for space explorations [3]. To name a few high-tech space telescopes which will in the near future provide us with a lot of new data, one cannot go without mentioning the James Webb and Nancy Grace Roman Space Telescopes [4, 5]. Therefore, we are expecting new and more accurate details about these perplexing objects in the following years.

Furthermore, studying brown dwarfs allows us also to test modified theories of gravity. Before obtaining this new data from future missions, one can model the cooling processes of brown dwarfs in different theories of gravity. Utilising the received results it will be possible to constrain and maybe in some cases to rule out some theories. It has already been established that the cooling processes do indeed depend on the gravity [6]. This conclusion is useful, since theoreticians have proposed many alternatives to general relativity (GR) theory, which should be tested with all possible tools. GR has been proven to give accurate descriptions about the Solar System [7] and many other gravitational phenomena, such as the existence of black holes [8, 9] and gravitational waves [10].

However, there are still some occurrences, such as dark matter, which is mainly indicated by the shape of the galaxies' rotation curves [11, 12], and dark energy which is responsible for the accelerated expansion of the Universe [13] that GR cannot explain. This is one of the reasons why one searches for alternatives and studies modified gravity. One of the proposed modified theories is Horndeski theory of gravity [14].

In this work, we will investigate how non-relativistic Horndeski theory affects the cooling process of brown dwarfs in comparison to Newtonian one. Formulae for different brown dwarfs' quantities are derived in Horndeski gravity. Employing a numerical approach we obtain the solutions to these equations.

In the first and second chapter, previous studies based on Newtonian gravity are presented. The third and fourth chapter include the derivations and results which were done by the author. One must keep in mind, that these are novel results and not have been published before. Therefore, they will be a part of the upcoming publication [15].

Chapter 1

Modelling substellar objects

The purpose of this chapter is to present the theoretical framework that is used to investigate substellar objects[1]. Here all of the topics and formulae from previous research on which the thesis is based on are thoroughly explained. Therefore, we will recall here the well-known description of the brown dwarf stars in Newtonian gravity such that it will allow us to move smoothly to the analogous formalism but based on Horndeski gravity instead. Firstly, we introduce the definition and basic notions related to brown dwarfs. Secondly, we will focus on how one can describe the interior of a substellar object: that is, an equation of state, hydrostatic equilibrium equation and derived from it, the Lane-Emden equation. Lastly, a procedure which will allow to model atmospheric properties in a simple way will be introduced.

Let us underline that the presented formalism allowing to describe substellar objects is based on Newtonian gravity. In the further part we will present the Horndeski analogue.

1.1 Brown dwarfs

Brown dwarfs (BDs) are a class of substellar objects [16]. The prefix '*sub-*' comes from Latin and means 'under' [17]. In astrophysics, the word 'substellar' describes a an astrophysical object which mass is smaller than the critical mass needed to start stable nuclear reactions during which hydrogen is fused into helium [16]. It was first suggested by A. S. Eddington that stars get their energy from hydrogen-helium fusion or proton-proton chain [18]. Later it was proved that this could indeed provide the immense amount of energy needed to keep a stellar object stable [19]. Now we know that such nuclear fusion reactions are indeed the source of a main-sequence star's energy, but a critical mass is needed in order to achieve high enough

[1]Since we are mainly focused on brown dwarf stars, we will use the notions 'a substellar object' and 'a brown dwarf star' as synonyms.

temperatures and pressures for them to occur [20]. When an astrophysical object does not have sufficient mass to sustain stable hydrogen-helium fusion, it is named a substellar object. Other nuclear reactions might still take place in such objects, but they are different from reactions powering main-sequence stars [16]. It has been estimated by different models that the minimal mass for hydrogen-helium fusion is about $0.064M_\odot$ - $0.0874M_\odot$, where $M_\odot$ denotes the Sun's mass [21].

However, brown dwarfs can still have nuclear fusion reactions occurring in their core. Some have the mass needed for deuterium fusion to occur but not enough for hydrogen-helium[2]. The minimal mass needed for deuterium fusion is estimated to be about 0.012 $M_\odot$. Still, there exist brown dwarfs in which no nuclear fusion takes place, therefore, these reactions do not set the lower mass limit for brown dwarfs. [23]

The way to differentiate between BDs and planets is to analyse their formation processes. Like light main-sequence stars, brown dwarfs also form from a collapsing gas cloud. This has been already confirmed by observations [24]. A gas cloud starts to collapse when a disturbance compresses the gas beyond a critical value - this is called the Jeans instability. The gas starts contracting due to gravity and a dense protostar forms [25]. Both brown dwarf stars and low-mass main-sequence stars form this way. However, planets form around those protostars from material left over from the star. The critical mass separating BDs from giant planets is called opacity mass and it is the lowest mass that a gas cloud can have without crumbling into smaller pieces only due to gravitational instabilities. This critical mass is about $0.003M_\odot$ [26].

Therefore the mass of a brown dwarf has to be between $0.003M_\odot$ and $0.087M_\odot$.

1.2 Equations of state for substellar objects

In order to describe a microscopic system in terms of macroscopic variables, an equation of state (EoS) must be given. Generally speaking, it represents the thermodynamic processes occurring in the system being in the statistical equilibrium state [27]. Depending on a kind of particles which our system consists of, and interactions between them, there are many of such equations of state which relate thermodynamic variables to each other. The most popular EoS used in stellar modelling with a simple relation between the pressure p inside the object and the energy density ρ is given by the barotropic relation [28]

$$p = p(\rho)\ . \tag{1.1}$$

[2] Deuterium fusion is another kind of nuclear reaction than hydrogen to helium. In the first case, the produced nucleus is ^{3}He, while in the second one ^{4}He. Thus, the deuterium fusion requires lower temperatures and pressures and consequently, the critical mass for reactions to start is also lower than in the case of hydrogen-helium fusion. [22]

In astrophysics, one needs to consider which thermodynamic processes happen inside an object in order to produce an accurate EoS. For stellar, and consequently later for substellar objects, it was already derived and observed in late 1800s that they must be in convective and polytropic equilibrium [29]. Lord Kelvin has said that [29]

> ‘*If a gas is enclosed in a rigid spherical shell impermeable to heat and left to itself for a sufficiently long time, it settles into the condition of gross-thermal equilibrium by "conduction of heat" till the temperature becomes uniform throughout. But if it were stirred artificially all through its volume, currents not considerably disturbing the static distribution of pressure and density will bring it approximately to what I have called convective equilibrium of temperature. The natural stirring produced in a great free fluid mass like the Sun's by the cooling at the surface, must, I believe, maintain a somewhat close approximation to convective equilibrium throughout the whole mass.*’

It can be shown that in the case of a convective interior the barotropic equation of state takes the form of a polytrope [29]:

$$p = K\rho^{\gamma} , \tag{1.2}$$

where γ is defined as $\gamma = \frac{C_p}{C_v}$, where C_p is the isobaric thermal capacity while C_V is the isochoric thermal capacity. In most cases, γ is a constant parameter, which value provides a class of the considered object. For instance, $\gamma = \frac{5}{3}$ corresponds to astrophysical objects in non-relativistic cases, while $\gamma = \frac{4}{3}$ to relativistic cases [28]. Here, the parameter K includes different information about the interactions between particles, which will be discussed in a further part. In the simplest model, given by Chandrasekhar, it is assumed that K is a constant depending on the type of an astrophysical object [29].

Usually, a more convenient form of polytropic EoS is used when the parameter n is introduced

$$n = \frac{1}{\gamma - 1} , \tag{1.3}$$

such that the EoS (1.2) can be written as

$$p = K\rho^{1+\frac{1}{n}} . \tag{1.4}$$

This allows us to write down the Lane-Emden equation in a more elegant form as seen in the section 1.3.

On the other hand, the atmosphere and photosphere of an astrophysical object considered here are modelled using an ideal gas approximation. Hence, the ideal gas equation of state in the following form is used

$$pV = \frac{m}{\mu}RT \ , \tag{1.5}$$

where V is volume, m mass of the gas, μ molar mass of the gas, R ideal gas constant and T temperature [30].

1.2.1 The internal properties of brown dwarfs

Since the brown dwarfs are less massive than main-sequence stars they do not have sufficient conditions in the core to fuse hydrogen into helium-4. In the main-sequence stars this nuclear reaction produces enough radiation pressure to balance the gravitational contraction, which lead to a stable object. On the contrary, since brown dwarfs do not have such an energy source the matter is so compressed that it becomes degenerate. Furthermore, such matter is well approximated by the non-relativistic electron gas which is given by the polytropic EoS (1.2) with $\gamma = \frac{5}{3}$ [21]

$$p = K\rho^{\frac{5}{3}} \ . \tag{1.6}$$

The matter inside substellar objects behaves differently than in main-sequence stars or planets, thus, the parameter K in the EoS must be appropriate for brown dwarfs. Using a model proposed by S. Auddy, S. Basu and S. R. Valluri [21], one considers that inside brown dwarfs there is a balance between gravity and the pressure produced by the electron degeneracy and ionised gas. Meaning, the EoS includes the pressure of a degenerate Fermi gas and the pressure due to ions. Thus, instead of K being a constant parameter in equation (1.2) like in the Chandrasekhar case, the recent models treat it as dynamical, since it contains a time dependant term - electron degeneracy. For brown dwarfs:

$$K = C\mu_e^{-5/3}(1 + b + a\Psi) \ , \tag{1.7}$$

where

$$b = -\frac{5}{16}\Psi \ln\left(1 + e^{-\frac{1}{\Psi}}\right) + \frac{15}{8}\Psi^2\left\{\frac{\pi^2}{3} + Li_2\left(-e^{-\frac{1}{\Psi}}\right)\right\} \tag{1.8}$$

and Ψ is the degeneracy parameter, which is defined as

$$\Psi = \frac{k_B T}{\mu_F} = \frac{2m_e k_B T}{(3\pi^2\hbar^3)^{2/3}}\left[\frac{\mu_e}{\rho N_A}\right]^{2/3} \ . \tag{1.9}$$

The meaning of the other quantities are given in Table 1.1

symbol	meaning/value
C	10^{13} cm^{4}g$^{-2/3}$s^{-2}
μ_e	$\frac{1}{\mu_e} = X + \frac{Y}{2}$ is the number of baryons per electron
X	the mass fraction of hydrogen
Y	the mass fraction of helium
a	$\frac{5\mu_e}{2\mu_1} = const.$
μ_1	the mean molecular weight for helium and ionized hydrogen mixture: $\frac{1}{\mu_1} = \left((1+x_{H^+})X + \frac{Y}{4}\right)$
x_{H^+}	the ionization fraction of hydrogen
k_B	the Boltzmann constant
T	temperature
μ_F	the electron Fermi energy in the degenerate limit
Li_2	polylogarithm function $Li_s(x) = \sum_{k=1}^{\infty} \frac{x^k}{k^s}$
m_e	the electron mass
$\hbar$	$\frac{h}{2\pi}$ is reduced Planck constant
h	the Planck constant
ρ	energy density
N_A	the Avogadro number

Table 1.1: Quantities in brown dwarf's equation of state [21]

It has to be noted here that the value of μ_1 depends on the model which describes the ionisation of the gas. The model is derived from entropy matching and in this work, we will be using model according to which [31]

$$x_{H^+} = 0.255\ . \tag{1.10}$$

Another quantity which we will need to take into account, since it is directly related to the used model, is the internal entropy S in the neighbourhood of the photosphere (the photosphere is discussed in the section 1.4). This can be derived using the first law of thermodynamics and the definition of the electron degeneracy parameter. It is given by [21]

$$S = \frac{3}{2}\frac{k_B N_A}{\mu_{1\text{mod}}}(\ln\Psi + 12.7065) + C_1 \tag{1.11}$$

where C_1 is the integration constant and

$$\frac{1}{\mu_{1\text{mod}}} = \left(\frac{1}{\mu_1} + \frac{3}{2}\frac{x_{H^+}(1-x_{H^+})}{2-x_{H^+}}\right). \tag{1.12}$$

1.3 The Lane-Emden equation

The Lane-Emden equation (LEE) was first derived in 1870 by J. H. Lane in his article 'On the Theoretical Temperature of the Sun' [32]. It was later analysed further by A. Ritter in 1878 and R. Emden in 1907 [33, 34]. Roughly speaking, it is a dimensionless Poisson equation, which for gravity is given as [35]

$$\nabla^2 \phi = 4\pi G\rho \ , \tag{1.13}$$

where ∇^2 is the Laplace operator, ϕ the scalar potential and G is the Newtonian gravitational constant. This equation describes gravitational potential sourced by the density ρ. Moreover, let us notice that in our case the gravitational field is static (time-independent). Introducing dimensionless parameters given below (equations (1.18) and (1.19)) yields the LEE. Its derivation is based on the hydrostatic equilibrium equation, which describes the balance between gravitational forces acting on the (sub)stellar object and internal pressure. In Newtonian physics the hydrostatic equilibrium equation has a following form [35]

$$\frac{dp(r)}{dr} = -\frac{Gm(r)\rho(r)}{c^2 r^2} \ , \tag{1.14}$$

where r is the radial distance from the object's centre, $p(r)$ is the pressure function depending on the radial distance, $m(r)$ is the mass function depending on the radial distance and c is the speed of light. The surface is defined by

$$p(r = R) = 0 \ , \tag{1.15}$$

where R is the radius of the object. In addition to this, the mass equation

$$m(r) = \int_0^r 4\pi r^2 \rho(r) dr \tag{1.16}$$

is necessary together with an appropriate EoS in order to fully define the system. Let us notice that $m(R) = M$ is defined to be the mass of the object. These are the main equations that describe a static, spherical-symmetric non-relativistic (sub)stellar object.

However, for our further purposes, it is more convenient to work with the Lane-Emden equation when one uses the polytropic equation of state [28]

$$\frac{1}{\xi^2}\frac{d}{d\xi}\left(\xi^3 \frac{d\theta}{d\xi}\right) + \theta^n = 0 \ , \tag{1.17}$$

where n is the polytropic index introduced in the previous subsection with the equation (1.3), and the dimensionless variables θ and ξ are defined as

$$\rho = \rho_c \theta(\xi)^n \qquad \text{and} \qquad p = p_c \theta(\xi)^{n+1} \tag{1.18}$$

and

$$r = r_c \xi \qquad \text{with} \qquad r_c^2 = \frac{p_c(n+1)}{4\pi G \rho_c^2}\,, \tag{1.19}$$

where ρ_c and p_c are central density and pressure respecively. The full derivation, boundary conditions and other features of the LEE are given in the appendix A.

Using the solutions from LEE one can derive the formulae for the mass M, radius R and central energy density ρ_c as [29]

$$M = 4\pi r_c^3 \rho_c \omega, \qquad R = \gamma_n \frac{K^{\frac{n-1}{n-3}}}{G}, \qquad \rho_c = \delta_n \frac{3M}{4\pi R^3}\,, \tag{1.20}$$

where the following parameter depend on the solution of the LEE (1.17)

$$\omega_n = -\xi^2 \frac{d\theta}{d\xi}\bigg|_{\xi=\xi_R}, \qquad \gamma_n = (4\pi)^{\frac{1}{n-3}} (n+1)^{\frac{n}{3-n}} \omega_n^{\frac{n-1}{3-n}} \xi_R\,, \qquad \delta_n = -\frac{\xi_R}{3 d\theta/d\xi|_{\xi=\xi_R}}\,. \tag{1.21}$$

1.4 The surface properties of brown dwarfs

There is no exact analytical model to properly describe the surface properties of stellar and substellar objects. Therefore, we will use the approximated analytical results provided by [31]. They used the matching procedure of the entropies obtained in the degenerate interior and in the radiative photosphere, where the last one is mainly characterised by the effective temperature. This allows to obtain the relation between effective temperature T_{eff}, the degeneracy parameter (1.9) and photsopheric pressure ρ_e in the form [31]

$$T_{\text{eff}}(\text{K}) = b_1 \times 10^6 \rho_e^{0.4} \Psi^{\nu}, \tag{1.22}$$

where b_1 and ν are numerical values depending on the specific model which was mentioned in (1.10). In the used model their values are [31]

$$b_1 = 2.00, \qquad \nu = 1.60. \tag{1.23}$$

From the equation (1.22), it is possible to derive the relation between the luminosity and the degeneracy parameter [21]. To do so, one uses the Stefan-Boltzmann equation, assuming a brown dwarf radiates energy as a black-body,

$$L = 4\pi R^2 \sigma T_{\text{eff}}^4 \ , \tag{1.24}$$

where L is the luminosity of the object, R is the radius of the object and σ is the Stefan-Boltzmann constant. Further, it will be demonstrated that the electron degeneracy Ψ is a function of time, thus, the luminosity and temperature are also time dependant, providing a cooling model for brown dwarfs [6].

In order to find the phostospheric density, let us notice that the surface gravity can be approximated as follows

$$g = \frac{Gm(r)}{r^2} \sim \frac{GM}{R^2} = const \ , \tag{1.25}$$

such that one can use it to rewrite the hydrostatic equilibrium equation (1.14) for Newtonian physics in the following form, which was first derived by A. Burrows and J. Liebert, [20]

$$\frac{dp}{dr} = -g\rho \ . \tag{1.26}$$

On the other hand, the photosphere is a visible layer in the atmosphere. It is defined by the optical depth $\tau = \frac{2}{3}$. Optical depth is given as [35]

$$\tau(r) = \kappa_R \int_r^\infty \rho dr \ , \tag{1.27}$$

where κ_R is the Rosseland mean opacity, which in the further parts will be assumed to be $\kappa_R = 0.01$ cm^2/g. This allows to analyse brown dwarfs' surface properties and derive the missing quantities to describe these objects.

It should be mentioned here that since some of the formulae are based on the hydrostatic equilibrium equation, which depends on the gravity theory, the final results will also be affected when a modified theory of gravity is introduced. This we will see in the next chapter.

Chapter 2

Modified gravity theories

General relativity (GR), which was first developed by A. Einstein in the beginning of the 20th century, is one of the best theories to describe gravitational systems in our Universe [36]. It predicts many phenomena with great accuracy - the most recent were the detection of gravitational waves produced by a merger of two black holes [37] and two neutron stars [38], and images of black holes [8, 9]. However, there are still some puzzles which GR cannot explain. These include dark matter problem, whose possible existence is mainly indicated by the flatness of the galaxies' rotation curves, as well as dark energy, that is, the accelerated expansion of our Universe. These yet inexplicable issues have led to investigate many alternatives to GR - modified theories of gravity. One of the most common model among various proposals of modifications to Einstein's gravity is a scalar-tensor theory[1]. It introduces a scalar degree of freedom, called the '5th force', whose dynamics provides the present cosmic acceleration [40] (dark energy), and it is also believed to be an agent of the early Universe's inflation. [41, 42, 43]

On the other hand, the effects of the scalar field are suppressed on a small scale by a screening mechanism, such that the theory is consistent with the Solar System tests [44]. In what follows, we will focus on the most general theory which admits a scalar degree of freedom and at the same time provides the second-order equations of motion for the metric and scalar field: Horndeski gravity [14]. We will also mention the generalisation of the Horndeski theory, which admits healthy solutions [45].

The Horndeski and beyond gravity turn out to be very useful to study cosmological problems, astrophysical objects, such as black holes and neutron starts [44], but also, as we will discuss soon, non-relativistic stars [46, 47] and substellar objects, which are our main concern.

[1] Let us notice that the most popular theory, $f(R)$ metric gravity, turn out to be a special case of a large scalar-tensor family [39].

2.1 Horndeski gravity and beyond

The Horndeski gravity is '*the most general scalar-tensor theory having second-order field equations in four dimensions*' [44]. Its gravitational part of the Lagrangian density has the following form:

$$\begin{aligned}\mathcal{L} = G_2(\phi,X) - G_3(\phi,X)\Box\phi + G_4(\phi,X)R + G_{4X}\left[(\Box\phi)^2 - \phi^{\mu\nu}\phi_{\mu\nu}\right] \\ + G_5(\phi,X)G^{\mu\nu}\phi_{\mu\nu} - \frac{G_{5X}}{6}\left[(\Box\phi)^3 - 3\Box\phi\phi^{\mu\nu}\phi_{\mu\nu} + 2\phi_{\mu\nu}\phi^{\nu\lambda}\phi^{\mu}_{\lambda}\right],\end{aligned} \tag{2.1}$$

where R is the Ricci scalar, $G_{\mu\nu}$ is the Einstein tensor, G_2, G_3, G_4, and G_5 are arbitrary functions of the scalar field ϕ, $X := -g^{\mu\nu}\nabla_\mu\phi\nabla_\nu\phi/2$ and $\phi_{\mu\nu} := \nabla_\mu\nabla_\nu\phi$. Here, ∇_μ denotes the covariant derivative and $\Box = \nabla^\mu\nabla_\mu$. [44]

The Lagrangian density (2.1) reduces to the Einstein-Hilbert one[2] when $G_4 =$ constant while other G_i, $i \in \{2,3,4X,5,5X\}$, are equalled zero.

There exists a generalisation of Horndeski gravity, the so-called degenerate higher-order scalar-tensor theories (DHOST) [45]. They also provide healthy solutions although the field equations includes higher derivatives of the field. This generalisation can also be divided into different classes [48], but since it is not a topic of this thesis, we will skip the discussion related to it.

However, what is more important, some classes of Horndeski gravity and beyond have been already shown not to be consistent with the constraint given by the speed of gravitational waves c_{GW} [49, 50].

The fact of the almost simultaneously detection of two neutron stars' merger GW170817 [10] and their gamma-ray burst GRB170817A [38] provides that [44]

$$-3\times10^{-15} < c_{\mathrm{GW}} - 1 < 7\times10^{-16}\ . \tag{2.2}$$

Therefore, one should focus on classes which satisfies the condition $c_{\mathrm{GW}} = 1$. For example, in the case of Horndeski gravity, only the following Lagrangian density satisfies this constraint [44]:

$$\mathcal{L} = G_2(\phi,X) - G_3(\phi,X)\Box\phi + G_4(\phi)R\ . \tag{2.3}$$

Apart from this, it should be mentioned that the effects of the scalar field, which is an alternative to dark energy and therefore plays an important role in cosmology, must be screened in the case of small scales [44]. In the Solar System the Einstein's gravity has been tested with high

[2]That is, the Lagrangian density of GR which has a form $\mathcal{L} = R$.

precision such that the dynamics of the scalar field must be suppressed there. The mechanism responsible for that is called a screening mechanism. The screening mechanism widely used in DHOST is Vainshtein one [51]. In the further part, we will focus on a special class of DHOST, called G^3-galileon [52].

2.2 Non-relativistic limit of Horndeski gravity for a spherical-symmetric case

It turns out that in the interiors of non-relativistic astrophysical objects such as stars and substellar objects, the Vainshtein mechanism is partially broken in the case of G^3-galileon models [46]. Therefore, when one considers the weak field limit of the beyond Horndeski theories, that is, we will consider that the scalar field can be expanded about its cosmological value ϕ_0: $\phi(r,t) = \phi_0(t) + \phi_1(r,t)$, while the spherical-symmetric ansatz for the metric has the standard form:

$$ds^2 = -(1+2\Phi(t,r))dt^2 + (1-2\Psi(t,r))dr^2 + r^2 d\Theta^2 + r^2 \sin^2(\theta) d\phi^2 \, , \tag{2.4}$$

where $\Phi(t,r)$ and $\Psi(t,r)$ are gravitational perturbations, also called gravitational potentials [46]. However, we are interested in a static case as for the most of the stellar evolution stars and substellar objects can be considered as static bodies. In order to obtain the non-relativistic equations[3], one inserts the perturbed form of the scalar field and metric into the modified Einstein's field equations and considers only the leading terms. This results as [46]

$$\begin{aligned} \frac{d\Phi}{dr} &= \frac{G_N M(r)}{r^2} + \frac{\Upsilon}{4} G_N M''(r) \\ \frac{d\Psi}{dr} &= \frac{G_N M(r)}{r^2} - \frac{5\Upsilon}{4} \frac{G_N M\prime(r)}{r} . \end{aligned} \tag{2.5}$$

where G_N is the Newtonian gravitational constant equalled to $G_N = G$, which was already introduced in the previous chapter 1, and Υ is a dimensionless parameter of the theory. It depends mainly on the time derivative of the cosmological term of the scalar field, that is, $\dot{\phi}_0$. It has been already constrained by the various studies [47, 53], therefore we will only consider the values from the range

$$-\frac{2}{3} < \Upsilon \lesssim 1.6. \tag{2.6}$$

[3]Let us notice that this procedure is beyond the topic of this thesis.

On the other hand, the Euler equations for a static, spherical symmetric non-relativistic object in general is given by [46]

$$\frac{1}{\rho}\frac{dp}{dr} = -\frac{d\Phi}{dr} \tag{2.7}$$

and hence the hydrostatic equilibrium equation can be obtained with the use of (2.5):

$$\frac{dp}{dr} = -\frac{G_N M(r)\rho(r)}{r^2} - \frac{\Upsilon}{4} G_N \rho(r) M''(r). \tag{2.8}$$

Moreover,

$$\frac{dM}{dr} = 4\pi r^2 \rho(r) \tag{2.9}$$

such that

$$\frac{d^2 M}{dr^2} = 8\pi r\rho + 4\pi r^2 \frac{d\rho}{dr} \tag{2.10}$$

can be used in the hydrostatic equilibrium equation (2.8). The modified Lane-Emden equation is obtained by the similar procedure given in the appendix A [46].

$$\frac{1}{\xi^2}\frac{d}{d\xi}\left[\left(1 + \frac{n}{4}\Upsilon\xi^2\theta^{n-1}\right)\xi^2\frac{d\theta}{d\xi} + \frac{\Upsilon}{2}\xi^3\theta^n\right] = -\theta^n \ . \tag{2.11}$$

One should note here that in this theory the mass M, radius R, radial coordinate r, density ρ and pressure p have the same forms as given in the previous section.

Chapter 3

Cooling model for brown dwarfs in Horndeski theory

In this chapter and the chapter 4 new results are presented. We will derive the equations needed to describe the internal and surface properties of a brown dwarf star in Horndeski theory. These formulae will allow to obtain the cooling model for such a substellar object in modified gravity. In order to do so, we will need to firstly derive how the electron degeneracy depends on time. The calculations are also going to appear in the up-coming publication [15].

3.1 Internal properties

It was already discussed in chapter 1 that the polytropic parameter n of equation of state for fully degenerate non-relativistic electrons takes the value $n = 1.5$. Therefore, to characterise brown dwarfs, we will consider an EoS in the following form

$$p(\rho) = K\rho^{\frac{5}{3}} , \tag{3.1}$$

where K is given by the equation (1.7). In order to obtain different parameters such as radius, central density, and pressure for brown dwarfs the formulae (1.20) with $n = 1.5$ were used. Thus, one gets

$$M = 4\pi r_c^3 \rho_c \omega, \qquad R = \gamma \frac{K}{GM^{1/3}}, \qquad \rho_c = \delta \frac{3GM^2}{4\pi\gamma^3 K^3} , \tag{3.2}$$

and

$$\omega = -\xi_R^2 \frac{d\theta}{d\xi}\bigg|_{\xi=\xi_r}, \qquad \gamma = \left[\frac{125}{128\pi^2}\right]^{1/3} \omega^{1/3}\xi_R, \qquad \delta = -\frac{\xi_R}{3d\theta/d\xi\big|_{\xi=\xi_R}} . \tag{3.3}$$

Hence, to find these parameters' values, the modified LEE (2.11) must be numerically solved, like it was discussed in section 1.3. Before doing that, formulae for brown dwarf's radius, central energy density, pressure and temperature still containing the mass M, degeneracy parameter Ψ and terms related to the LEE are derived. That means that one plugs the constants and K into the equations (1.20). The parameters are characterised in such a way in order to check the equations credibility, since analogous formulae have been derived already for Palatini gravity theory [54]. It has to be noted, that we are using the (centimetregramsecond) CGS unit system, since it is widely used among the astrophysical community such that it is easier to compare the results with Newtonian gravity. For the readers convince, we will provide the well known constants in this system of units:

$$\begin{aligned} G(\text{dyn cm}^2\text{g}^{-2}) &= 6.67430 \times 10^{-8} , \\ M_\odot(\text{g}) &= 1.989 \times 10^{33} , \\ L_\odot(\text{erg s}^{-1}) &= 3.839 \times 10^{33} , \end{aligned} \tag{3.4}$$

where the index '$\odot$' refers to Solar quantities, while K is

$$K(\text{cm}^4\ \text{g}^{2/3}\text{s}^{-2}) = C\mu_e^{-5/3}(1+b+a\Psi) = \mu_e^{-5/3}(1+b+a\Psi)\times 10^{13} . \tag{3.5}$$

The radius is obtained by inserting these quantities and constants into the equation (1.20)

$$\begin{aligned} R(\text{cm}) &= \frac{10^{13}}{6.67430\times 10^{-8}\cdot(1.989\times 10^{33})^{1/3}} \left(\frac{M_\odot}{M}\right)^{1/3} \gamma\mu_e^{-5/3}(1+b+a\Psi) \\ &\approx 1.19138\times 10^9 \gamma \left(\frac{M_\odot}{M}\right)^{1/3} \mu_e^{-5/3}(a\Psi+b+1) , \end{aligned} \tag{3.6}$$

while central density and central pressure are expressed, respectively as

$$\begin{aligned} \rho_c(\text{g cm}^{-3}) &= 2.808007\times 10^5 \frac{\delta}{\gamma^3}\left(\frac{M}{M_\odot}\right)^2 \frac{\mu_e^5}{(a\Psi+b+1)^3} , \\ p_c(\text{Mbar}) &= 1.204103\times 10^{10} \frac{\delta^{5/3}}{\gamma^5}\left(\frac{M}{M_\odot}\right)^{10/3} \frac{\mu_e^{20/3}}{(a\Psi+b+1)^4} . \end{aligned} \tag{3.7}$$

The expression for central temperature can be derived from the definition of the electron degeneracy parameter (1.9). Hence, one can write

$$T_c = \frac{\Psi(3\pi^2\hbar^3)^{2/3}}{2m_e k_B}\left(\frac{\rho_c N_A}{\mu_e}\right)^{2/3}, \tag{3.8}$$

where ρ_c was derived previously, while constants are given as follows:

$$\begin{aligned} k_B(\mathrm{cm^2\ g\ s^{-2}\ K^{-1}}) &= 1.380649\times10^{-16} \\ N_A &= 6.02214076\times10^{23} \\ m_e(\mathrm{g}) &= 9.10938356\times10^{-28} \\ \hbar(\mathrm{cm^2\ g\ s^{-1}}) &= 1.0546\times10^{-27}\ . \end{aligned} \tag{3.9}$$

Furthermore, by inserting the numerical constants and ρ_c into the expression for central temperature, we obtain

$$T_c(\mathrm{K}) = 1.294057\times10^9\frac{\delta^{2/3}}{\gamma^2}\left(\frac{M}{M_\odot}\right)^{4/3}\frac{\Psi\mu_e^{8/3}}{(a\Psi+b+1)^2}\ . \tag{3.10}$$

Having already derived the analytical formulae for brown dwarf's internal parameters, we will move to the part describing the surface properties.

3.2 Surface properties

As discussed in the section 1.4, we can assume that on the surface the surface gravity is constant, thus

$$g = \frac{Gm(r)}{r^2} \sim \mathrm{const}\ , \tag{3.11}$$

such that $\frac{dg}{dr} = 0$. The modified hydrostatic equilibrium equation (2.8)

$$\frac{dp}{dr} = -\frac{Gm\rho}{r^2} - \frac{\Upsilon}{4}G\rho\frac{d^2m}{dr^2}\ , \tag{3.12}$$

can be rewritten using the derivatives

$$\frac{d}{dr}\left(\frac{Gm}{r^2}\right) = 0\ , \qquad \text{which gives} \qquad \frac{dm}{dr}\frac{1}{r^2} - 2\frac{m}{r^3} = 0\ . \tag{3.13}$$

Hence,

$$\frac{dm}{dr} = \frac{2m}{r} \qquad \text{and} \qquad \frac{d^2m}{dr^2} = \frac{2m}{r^2}. \tag{3.14}$$

Therefore, one can write the hydrostatic equilibrium equation for Horndeski gravity as

$$\frac{dp}{dr} = -\frac{Gm(r)}{r^2}\rho - \frac{\Upsilon}{2}\frac{Gm(r)}{r^2}\rho = -g\rho\left(1+\frac{\Upsilon}{2}\right) . \tag{3.15}$$

Using the definition of the photosphere $\tau = \frac{2}{3}$, where τ is given by (1.27)

$$\tau(r) = \kappa_R \int_r^\infty \rho dr = \frac{2}{3} \tag{3.16}$$

one can insert the density from the hydrostatic equilibrium equation (3.15)

$$\rho = -\frac{1}{g}\left(1+\frac{\Upsilon}{2}\right)^{-1}\frac{dp}{dr} \tag{3.17}$$

into the relation (3.16)

$$\frac{2}{3} = -\frac{\kappa_R}{g}\left(1+\frac{\Upsilon}{2}\right)^{-1}\int_r^\infty dp \tag{3.18}$$

to get the photospheric pressure by the above integration ($r \approx R$)

$$p_{\mathrm{ph}} = \frac{2GM}{3\kappa_R R^2}\left(1+\frac{\Upsilon}{2}\right) . \tag{3.19}$$

Inserting the radius (3.6), constant G and using the solar mass $M_\odot = 1.989\times10^{33}$ g, one can write

$$p_{\mathrm{ph}}(\mathrm{bar}) = \frac{62.352023}{\kappa_R\gamma^2}\left(\frac{M}{M_\odot}\right)^{5/3}\frac{\mu_e^{10/3}}{(a\Psi+b+1)^2}\left(1+\frac{\Upsilon}{2}\right) . \tag{3.20}$$

Combining the relation between effective temperature, degeneracy parameter and photospheric pressure (1.22) with the ideal gas law (1.5), we get that

$$p_{\mathrm{ph}}V_{\mathrm{ph}} = p_{\mathrm{ph}}\frac{m}{\rho_{\mathrm{ph}}} = \frac{m}{\mu_2}N_A k_B T_{\mathrm{eff}} , \tag{3.21}$$

where μ_2 is the mean molecular weight for the hydrogen and helium mixture in the photosphere and $\frac{1}{\mu_2} = \frac{X}{2} + \frac{Y}{4}$. Thus,

$$\rho_{\mathrm{ph}} = \frac{p_{\mathrm{ph}}\mu_2}{N_A k_B T_{\mathrm{eff}}} . \tag{3.22}$$

Using the effective temperature formula (1.22) one can write the photospheric density as

$$\rho_{\mathrm{ph}} = \frac{T_{\mathrm{eff}}^{5/2}}{b_1^{5/2}\times10^{15}\Psi^{5\nu/2}} . \tag{3.23}$$

Substituting this into (3.22) gives

$$\frac{T_{\text{eff}}^{5/2}}{b_1^{5/2}\times 10^{15}\Psi^{5\nu/2}} = \frac{p_{\text{ph}}\mu_2}{N_A k_B T_{\text{eff}}} . \tag{3.24}$$

Therefore, the one writes the effective temperature as a function of the electron degeneracy Ψ

$$T_{\text{eff}} = \frac{p_{\text{ph}}^{2/7}\mu_2^{2/7}b_1^{5/7}\times 10^{30/7}\Psi^{5\nu/7}}{N_A^{2/7}k_B^{2/7}} . \tag{3.25}$$

One can assume that the mass fractions of hydrogen and helium respectively are about 0.75 and 0.25, thus, $\mu_2 \approx 2.286$. Substituting the constants which have already been defined in the previous section by (3.9), μ_2 and the photospheric pressure p_{ph} with (3.20), gives

$$T_{\text{eff}}(K) = \frac{2.557879\times 10^4}{\kappa_R^{2/7}\gamma^{4/7}}\left(\frac{M}{M_\odot}\right)^{10/21}\frac{b_1^{5/7}\Psi^{\nu\cdot 5/7}}{(a\Psi+b+1)^{4/7}}\left(1+\frac{\Upsilon}{2}\right)^{2/7} . \tag{3.26}$$

Finally, we are able to calculate luminosity using the Stefan-Boltzman law (1.24), which allows one to write the luminosity as a function of the degeneracy parameter

$$L = \frac{0.072233L_\odot}{\kappa_R^{8/7}\gamma^{2/7}}\left(\frac{M}{M_\odot}\right)^{26/21}\frac{b_1^{20/7}\Psi^{\nu\cdot 20/7}}{(a\Psi+b+1)^{2/7}}\left(1+\frac{\Upsilon}{2}\right)^{8/7} , \tag{3.27}$$

where $\sigma = 5.6704\times 10^{-5}$ g s^{-3}K^{-4} and $L_\odot = 3.839\times 10^{33}$ erg s^{-1}. However, the electron degeneracy is a function of time, therefore, in the next section, we will derive the time evolution of this quantity.

3.3 Cooling process

In this section we are going to study a simple cooling model. Hence, the first and second law of thermodynamics will be used, in order to derive how the energy of a contracting star is changing. Following [20] the energy equation is given by

$$\frac{dE}{dt} + p\frac{dV}{dt} = T\frac{dS}{dt} = \dot{\varepsilon} - \frac{\partial L}{\partial M} , \tag{3.28}$$

where t is time, S the entropy per mass, E the energy and $\dot{\varepsilon}$ is the energy generation, which we can ignore in the brown dwarfs. From integrating this equation with respect to the mass, one gets that

$$\frac{ds}{dt}\left[\int N_A k_B T dM\right] = -L \ , \tag{3.29}$$

where $s = S/k_B N_A$. Here, it is possible to replace the mass with relation

$$M = V\rho \Rightarrow dM = \rho dV \ , \tag{3.30}$$

while T can be substituted using the electron degeneracy parameter definition (1.9)

$$T = \frac{\Psi(3\pi^2\hbar^3)^{2/3}}{2m_e k_B}\left(\frac{\rho N_A}{\mu_e}\right)^{2/3} \ . \tag{3.31}$$

Then one sees that

$$\frac{ds}{dt}\left[\int N_A \frac{\Psi(3\pi^2\hbar^3)^{2/3}}{2m_e}\left(\frac{N_A}{\mu_e}\right)^{2/3} \rho^{5/3} dV\right] = -L \ . \tag{3.32}$$

From the polytropic EoS, it is known that

$$p = K\rho^{5/3} = C\mu_e^{-5/3}(1+b+a\Psi)\rho^{5/3} \ , \qquad \text{thus,} \qquad \rho^{5/3} = \frac{p\mu_e^{5/3}}{C(1+b+a\Psi)}. \tag{3.33}$$

Furthermore, one can now subtitute this into (3.32) and get

$$\frac{ds}{dt}\left[\frac{N_A \Psi A \mu_e}{C(1+b+a\Psi)}\int p dV\right] = -L \ , \tag{3.34}$$

where A is defined as $A = \frac{(3N_A\pi^2\hbar^3)^{2/3}}{2m_e}$. Recalling from [35] that

$$\int p dV = \frac{2}{7}\frac{GM^2}{R} \ , \tag{3.35}$$

one can write that

$$\frac{ds}{dt}\left[\frac{2N_A \Psi A \mu_e}{7C(1+b+a\Psi)}\frac{GM^2}{R}\right] = -L \ . \tag{3.36}$$

Now one can use the time variation of entropy (1.11) to obtain that

$$\frac{ds}{dt} = \frac{1.5}{\mu_{1\text{mod}}}\frac{1}{\Psi}\frac{d\Psi}{dt} \ , \tag{3.37}$$

following the procedure presented in [21]. This allows to derive the time evolution of the degeneracy parameter

$$\frac{d\Psi}{dt} = \frac{ds}{dt}\frac{\Psi\mu_{1\text{mod}}}{1.5} \ . \tag{3.38}$$

The next step is to substitute $\frac{ds}{dt}$ with the relation (3.36). One gets that

$$\frac{d\Psi}{dt} = -L\left[\frac{7C(1+b+a\Psi)}{2N_A\Psi A\mu_e}\frac{R}{GM^2}\right]\frac{\Psi\mu_{1\mathrm{mod}}}{1.5}\ . \tag{3.39}$$

By plugging the radius given by the formula (3.6) and numerical values for the constants into the above equation, finally we obtain that the time evolution of the degeneracy parameter can be written as

$$\frac{d\Psi}{dt} = \frac{-1.018097\times 10^{-18}\mu_{1\mathrm{mod}}}{\kappa_R^{8/7}}\left(\frac{M_\odot}{M}\right)^{23/21}\frac{b_1^{20/7}\Psi^{\nu\cdot 20/7}(a\Psi+b+1)^{12/7}}{\mu_e^{8/3}}\left(1+\frac{\Upsilon}{2}\right)^{8/7}\ . \tag{3.40}$$

This equation together with (3.27) are the main results of this thesis. In the next section, we will focus on solving this equation numerically.

It has to be noted here that all of the final equations were checked with respect to the units.

Chapter 4

Numerical solutions

In the previous chapter we focused on the analytical cooling model describing brown dwarfs, however, in order to obtain the time evolution for the luminosity one must numerically solve the differential equations (3.40) and (3.27) with the modified Lane-Emden equation (2.11). Numerical solutions and figures with the time evolution of the electron degeneracy parameter as well as luminosity will be presented in this chapter.

4.1 Solving the modified Lane-Emden equation

As one can see in the equation (3.27), the expression describing luminosity contains the term with γ which is related to the solution of the modified LEE (2.11) by the definition (3.3). Therefore, since brown dwarf stars are described by $n = 1.5$ for which the modified LEE does not have any exact solution, we have to follow a numerical approach. This can be done using various programming languages and libraries. In this work, Python, together with Jupyter Notebook, is used to obtain the numerical solutions. In order to plot the solutions, the library Matplotlib is employed. The code solving the LEE for $n = 1.5$ and plotting the functions for different Υ values is presented in appendix B. The range of the parameter Υ was already discussed in chapter 2.2. We chose specific values within this range with interval $[0.3]$. The resulting graph is presented in the figure 4.1 below.

From the numerical solutions, one is also able to compute the following parameters for different Υ values

$$\omega = -\xi_R^2 \frac{d\theta}{d\xi}\bigg|_{\xi=\xi_r}, \qquad \gamma = \left[\frac{125}{128\pi^2}\right]^{1/3} \omega^{1/3}\xi_R, \qquad \delta = -\frac{\xi_R}{3d\theta/d\xi\big|_{\xi=\xi_R}}. \tag{4.1}$$

Their values are given in Table 4.1.

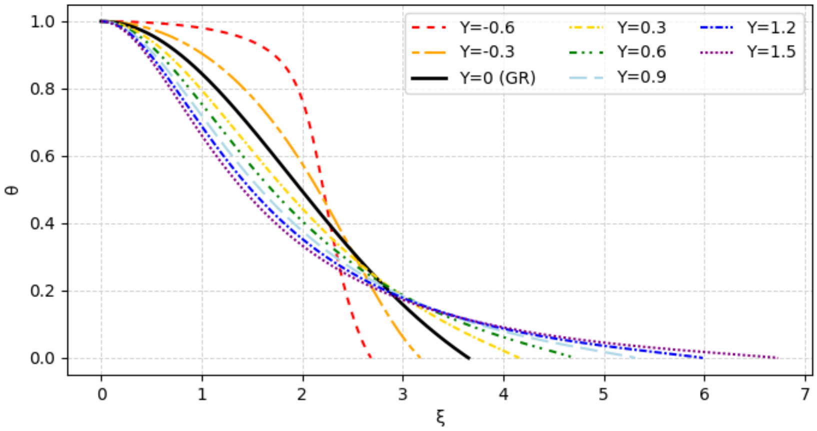

Figure 4.1: Numerical solutions of the modified Lane-Emden equations (2.11) for different Υ values

Υ	ξ_r	ω	γ	δ
-0.6	2.684	3.108	1.812	2.075
-0.3	3.176	2.822	2.076	3.785
0 (GR)	3.654	2.714	2.357	5.991
0.3	4.159	2.664	2.667	9.004
0.6	4.708	2.650	3.013	13.126
0.9	5.312	2.645	3.398	18.890
1.2	5.983	2.651	3.830	26.926
1.5	6.733	2.684	4.328	37.905

Table 4.1: Key parameter values for different Υ related to the solutions of modified LEE.

4.2 Solving for the electron degeneracy parameter and luminosity

In order to obtain the time evolution of the luminosity which depends on the parameter Υ, the differential equation

$$\frac{d\Psi}{dt} = \frac{-1.018097\times10^{-18}\mu_{1\mathrm{mod}}}{\kappa_R^{8/7}}\left(\frac{M_\odot}{M}\right)^{23/21}\frac{b_1^{20/7}\Psi\nu\cdot^{20/7}(a\Psi+b+1)^{12/7}}{\mu_e^{8/3}}\left(1+\frac{\Upsilon}{2}\right)^{8/7} \tag{4.2}$$

must be solved. It is not possible to find an exact analytical solution, thus, one must use a numerical method. In addition to Matplotlib, another library Scipy is used to obtain the results. In Scipy's package 'integrate' one can find a function 'odeint', which can be used to solve an ordinary differential equation. Utilising this in our code and defining functions for the electron degeneracy parameter, which is presented in appendix C, one gets the numerical solution describing the time evolution of the degeneracy parameter. This solution consists of data points, which provide the information about the values of the degeneracy parameter for different Υ values at predefined time points. We chose our initial time to be 10^6 years after the start of the formation of the brown dwarf, since by then, we assume that the brown dwarf is fully formed. The endpoint is arbitrary, but in order to be consistent with the age of the Universe ($\approx 14 \times 10^9$ years) and currently observable brown dwarfs, 10^{10} years is a reasonable choice.

To numerically obtain the luminosity, one needs to plug the specific values of the degeneracy parameter into the equation (3.27). This can be done, by defining a function, which is presented in appendix C. As a result, we get the luminosity values for different Υ values at the same predefined time points as the electron degeneracy parameter.

4.3 Comparing the code with previous resources

We also want to make sure that the results that one gets with our code match the previous works done in the field. In order to do this, the time evolution of the degeneracy parameter Ψ and luminosity for general relativity ($\Upsilon = 0$) are found. Our results for GR are compared to the figures given in [6].

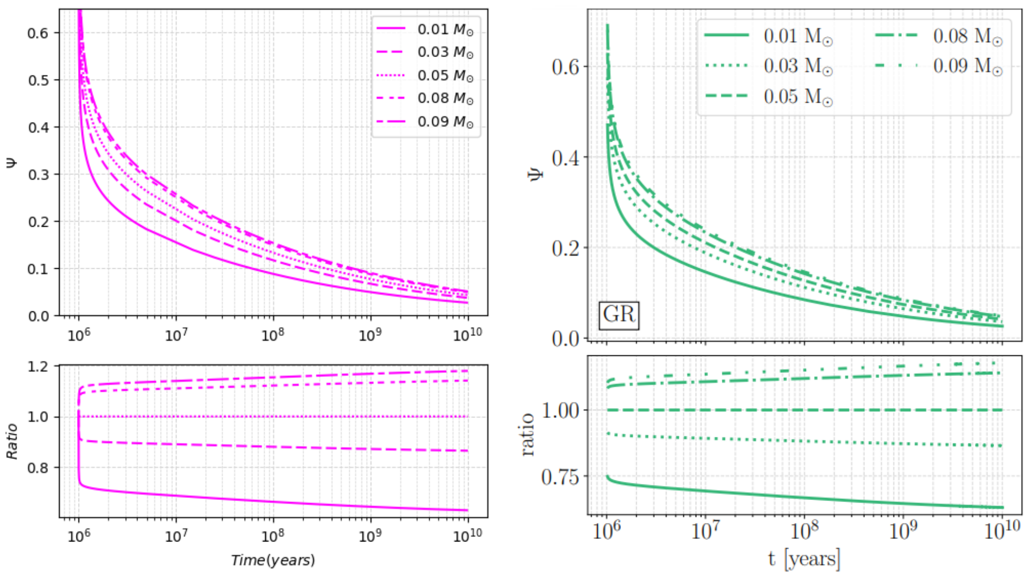

Figure 4.2: Electron degeneracy as a function of time given by the equation (3.40) where the horizontal axis is in the logarithmic scale to better distinguish the differences. The left graph (pink) is a result obtain in the thesis and the right graph (green) is taken from [6].

The same comparison as above, but for the luminosity evolution is given in the figure 4.3 below.

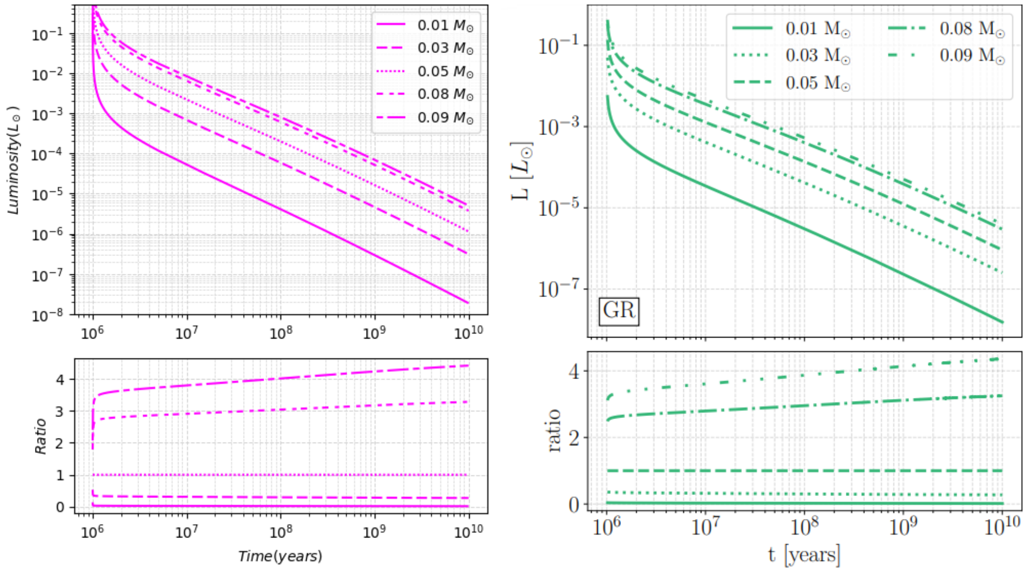

Figure 4.3: Luminosity as a function of time given by the equation (3.27) where the horizontal axis is in the logarithmic scale to better distinguish the differences. The left graph (pink) is a result of the thesis and the right graph (green) is taken from [6].

Therefore, we can conclude that the codes presented in appendix B and appendix C are valid and give results consistent with previous research.

4.4 Solutions for Horndeski theory of gravity

Having defined the functions for the electron degeneracy parameter as well as luminosity, one can use the numerical results obtained by solving the modified Lane-Emden equation. However, one variable is still undefined: the mass of the brown dwarfs. In our approach, the BD's mass is treated as a parameter with the value taken from the range $0.87M_\odot - 0.003M\odot$, which was discussed in chapter 1. We chose the mass to be $0.05M_\odot$ similarly to [6]. Now, we have all the information needed to solve the time evolution of the degeneracy parameter and luminosity. The results describing the time dependence of the degeneracy parameter are presented in figure 4.4, while the evolution of the luminosity is given in the picture 4.5.

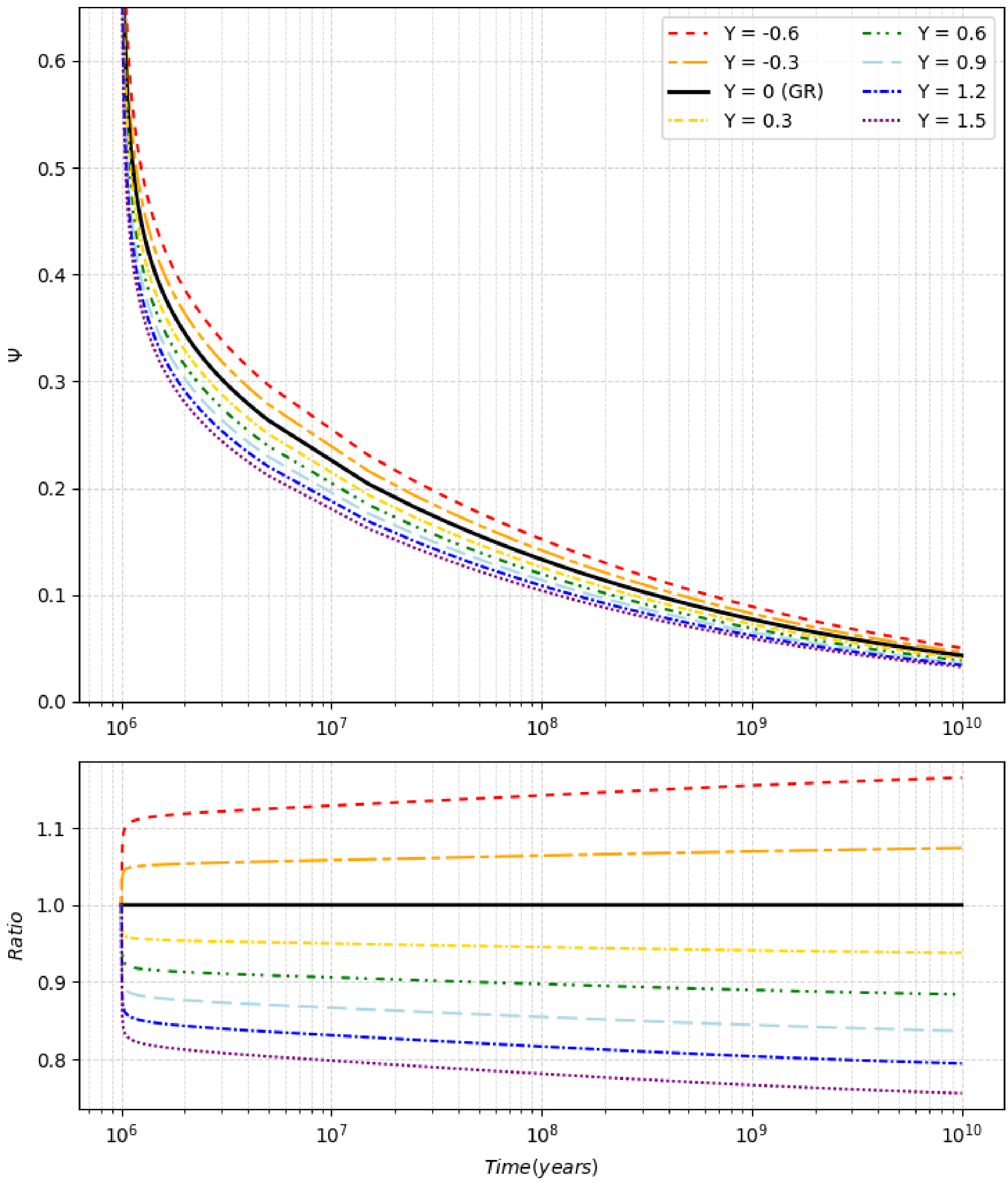

Figure 4.4: The time evolution of the electron degeneracy parameter Ψ in Horndeski gravity of a brown dwarf with the mass $0.05M_{\odot}$. The GR case is described by a thick black line, while $\Upsilon \neq 0$ corresponds to the considered modified gravity and is depicted by dashed lines. The scale is logarithmic to better demonstrate the differences. Lower graph shows the ratio between GR and different Υ values.

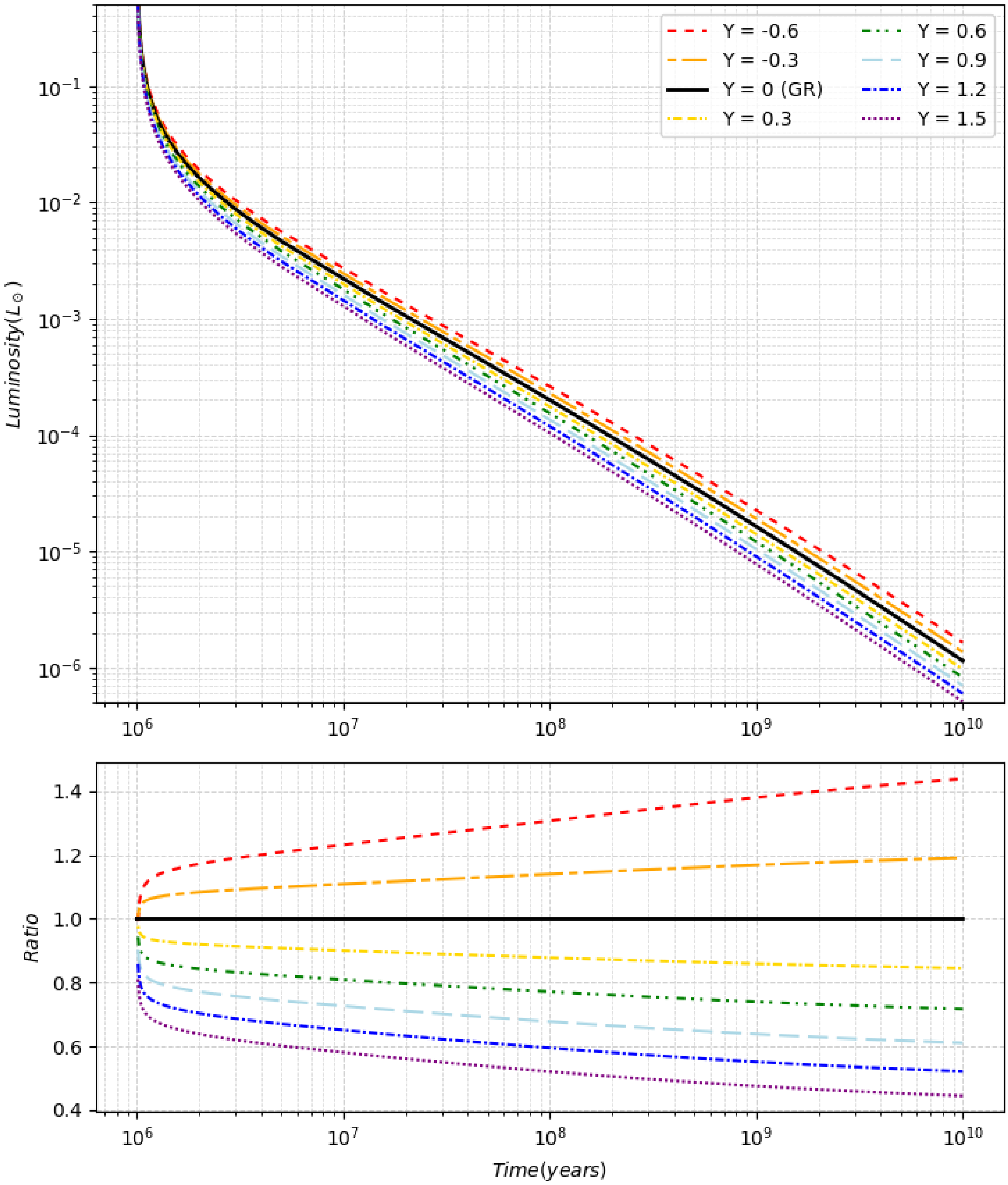

Figure 4.5: The time evolution of the luminosity in the solar luminosity $L_\odot$ in Horndeski gravity of a brown dwarf with the mass $0.05M_\odot$. The GR case is described by a thick black line, while $\Upsilon \neq 0$ corresponds to the considered modified gravity and is depicted by dashed lines. The scale is logarithmic to better demonstrate the differences. Lower graph shows the ratio between GR and different Υ values.

4.5 Results and discussion

We see from our figures 4.2 and 4.3 that in the case of Newtonian gravity ($\Upsilon = 0$) the curves coincide with previous studies [6, 21]. The obtained solutions are given for different masses from the range $0.01M_\odot - 0.09M_\odot$. It should be noticed that the curves with masses above $\sim 0.07M_\odot$ describe main-sequence stars. It can be seen that for greater masses one deals with longer evolution of the electron degeneracy parameter, thus, the astrophysical object remains brighter for an extended amount of time. This is in agreement with the equation (3.27), meaning, the numerical solutions do not only match previous research done in the field, but also with formulae derived in chapter 3.

One the other hand, let us comment that the solutions depicted in the graphs 4.2 and 4.3 were intended to confirm that the method developed in this theses does indeed work. The actual novel results about the cooling process of brown dwarfs in Horndeski gravity are presented in the figures 4.4 and 4.5.

In the picture 4.4 we see that greater modifications (the bigger absolute value of Υ) lead to substantial differences between non-relativistic Horndeski theory of gravity and Newtonian one, which is the non-relativistic limit of GR. We can also conclude that with the negative Υ values, that is, stronger gravity, it takes much more time for the matter in brown dwarfs to become degenerate. In the figure 4.4 all the solutions approach asymptotically the maximum electron degeneracy, that is, $\Psi = 0$ in our definition of the electron degeneracy (1.9)[1]. For the negative Υ values, it takes longer to approach this line, thus, it takes more time to reach a certain temperature when compared to Newtonian gravity. It is expected that currently there are not any fully degenerate brown dwarfs, since it would take more time than the age of the Universe ($\approx 14 \times 10^9$ years). Very likely, any other theory of gravity which does not have a similar behaviour describing the evolution of the electron degeneracy (the cooling process) in brown dwarfs could be questionable.

Furthermore, in the picture 4.4 the lower graph representing the ratios depicts that the difference between Newtonian gravity ($\Upsilon = 0$) and modified cases ($\Upsilon \neq 0$) becomes more distinguishable with time. One sees that in the early stages (time $\approx 10^7$ years) of brown dwarf cooling the difference between the Newtonian gravity and the modified theory could maximally be about 20%, while in later stages (time $\approx 10^{10}$ years) the difference is already over 25%. Therefore the effect of the modified gravity becomes clearer for older brown dwarf stars.

[1] One can notice that we use the opposite definition compared to for example [20].

Now, comparing the picture 4.4 to the figure 4.5, one sees that the luminosity has a different behaviour than the electron degeneracy. Meaning, with the given time we do not see the luminosities approaching any asymptote[2]. We see that for negative Υ values, the luminosity dims slower. Furthermore, this demonstrates that for stronger gravity the cooling process is longer. This makes our results physical, since with stronger gravity matter can be further compressed. As a result, densities and pressures are higher, thus, the temperatures as well and the cooling is slower. It should be also noted that the luminosity carries errors, since it depends on many quantities such as the radius and the effective temperature, which can happen to be troublesome to determine. However, this goes beyond the topic of this thesis.

Consequently, as luminosity depends on more parameters containing the terms related to the modified gravity the differences between Newtonian gravity and modified theory, which one sees in the lower graph in the figure 4.5, are much greater than they were for the electron degeneracy in the picture 4.4. The differences between modified gravity and Newtonian one also become more distinguishable with time. In the early stages the difference could maximally be about 40%, while in later stages it evolves to be over 55%. This demonstrates that the age of brown dwarfs could be an excellent tool to constrain modified theories of gravity, since some models could predict objects with luminosities which compared to the observational data could only belong to those older than the Universe.

Let us notice that the graphs showcased depict a brown dwarf with the mass $0.05M_{\odot}$. The reason for it is that in the case of higher masses one can already reach the main sequence stars. On the other hand, lower mass brown dwarfs not to tend to have the differences between Horndeski and Newton gravity bigger than a few per cents. Moreover, the interiors of massive brown dwarfs are more interesting because of possible nuclear fusion reactions (deuterium and lithium) which we leave for the future work.

All of these results allow to determine how the non-relativistic limit of Horndeski theory of gravity modifies the way the brown dwarf stars cool down. This model gives us new information, which we can test against the observational data in the nearest future. Currently, brown dwarfs are still quite mysterious objects about which we do not have a lot of highly accurate observational data. With plans, such as 'Cosmic Vision 2015-2025' [3], and new space telescopes James Webb and Nancy Grace Roman [4, 5], we will obtain more information about their properties which can be used to constrain theories of gravity analysing the cooling process as it has been done in this work.

[2] In our timescale.

Conclusion

In this thesis the analytical model describing the cooling of brown dwarfs in Horndeski gravity was derived. This was done using the modified Lane-Emden equation as well as different equations of state characterising brown dwarfs. The latter can be divided into different approaches to depict the interior and the photosphere of the substellar objects under study. Roughly speaking, one needs to analyse the matter properties of different regions of the brown dwarf star. Combining different results derived in the chapter 3, we were able to provide how the electron degeneracy parameter changes with time. It was necessary, since the expression for luminosity contains this parameter. It allowed us to obtain the time evolution of the luminosity which characterises the cooling process of brown dwarfs in Horndeski theory of gravity.

The second important part was to numerically solve the analytically derived equations. This was done using programming language Python with various libraries. As a result, we obtained how the cooling process changes when the Horndeski theory parameter Υ is varied. This result can be used to constrain the theory parameter by the observational data from future plans such as European Space Agency's 'Cosmic Vision 2015-2025'.

The models derived in this work can be further improved. The biggest uncertainties are related to the atmospheric descriptions such as the effective temperature and the opacity. Furthermore, we can also derive more general models by not making some of the assumptions that were made in this thesis, such as not assuming a constant surface gravity nor spherical symmetry.

Another prosperous future project concerning the results of this thesis, is to estimate the properties of the observational sample needed to confirm the predictions our model gives. This means that one needs to provide the information how accurate the brown dwarf's measurements need to be in order to constrain our model of gravity. To sum up, the research related to the brown dwarf stars in modified gravity theories is a very prosperous topic and studies in this field will definitely continue.

Acknowledgements

Many thanks to Morten Piibeleht who compiled the document template which was used in this thesis. I would also like to thank Maria Benito whose code in C++ was the inspiration behind my numerical solutions. Finally, I am so grateful for my supervisor Aneta Wojnar. She was extremely helpful, motivating and I could not ask for a better supervisor.

Kärt Soieva

Bibliography

1. S. S. Kumar, 'Study of degeneracy in very light stars', *Astronomical Journal* 67, 579 (1962).
2. R. Rebolo, M. R. Zapatero Osorio, and E. L. Martín, 'Discovery of a brown dwarf in the Pleiades star cluster', *Nature* 377, 129–131 (1995).
3. European Space Agency, 'Cosmic Vision', `https://sci.esa.int/web/cosmic-vision/-/46510-cosmic-vision`, Online; accessed 20 May 2022.
4. National Aeronautics and Space Administration, 'James Webb Space Telescope', `https://www.jwst.nasa.gov/`, Online; accessed 20 May 2022.
5. National Aeronautics and Space Administration, 'Nancy Grace Roman Space Telescope', `https://roman.gsfc.nasa.gov/`, Online; accessed 20 May 2022.
6. M. Benito and A. Wojnar, 'Cooling process of brown dwarfs in Palatini f(R) gravity', *Physical Review D* 103, 064032 (2021).
7. C. M. Will, 'The Confrontation between General Relativity and Experiment', *Living Reviews in Relativity* 17 (2014).
8. K. Akiyama and Event Horizon Telescope Collaboration, 'First M87 Event Horizon Telescope Results. I. The Shadow of the Supermassive Black Hole', *Astrophys. J. Lett.* 875, L1 (2019).
9. K. Akiyama and Event Horizon Telescope Collaboration, 'First Sagittarius A* Event Horizon Telescope Results. I. The Shadow of the Supermassive Black Hole in the Center of the Milky Way', *Astrophys. J. Lett.* 930, L12 (2022).
10. The LIGO Scientific Collaboration and The Virgo Collaboration, 'GW170817: Observation of Gravitational Waves from a Binary Neutron Star Inspiral', *Phys. Rev. Lett.* 119, 161101 (2017).

11. L. Bergström, 'Non-baryonic dark matter: observational evidence and detection methods', *Reports on Progress in Physics* 63, 793–841 (2000).

12. S. Capozziello and M. D. Laurentis, 'The dark matter problem from f(R) gravity viewpoint', *Annalen der Physik* 524, 545–578 (2012).

13. H. Huterer and M. S. Turner, 'Prospects for probing the dark energy via supernova distance measurements', *Physical Review D* 60, 081301 (1999).

14. G. W. Horndeski, 'Second-order scalar-tensor field equations in a four-dimensional space', *International Journal of Theoretical Physics* 10, 363–384 (1974).

15. A. Kozak, K. Soieva, and A. Wojnar, 'Cooling process of substellar objects in scalar-tensor gravity', *arXiv:2205.12812* (2022).

16. J. A. Caballero, 'A review on substellar objects beyond the deuterium burning mass limit: planets, brown dwarfs or what?', *Geosciences* 8, 362 (2018).

17. O. M. Communication, 'Dictionary Latin-English', `https://www.online-latin-dictionary.com/latin-english-dictionary.php?lemma=SUB100`, Online; accessed 10 May 2022.

18. A. S. Eddington, 'The internal constitution of the stars', *Nature* 106, 14–20 (1920).

19. R. d. E. Atkinson and F. G. Houtermans, 'Zur Frage der Aufbaumöglichkeit der Elemente in Sternen', *Zeitschrift für Physik* 54, 656–665 (1929).

20. A. Burrows and J. Liebert, 'The science of brown dwarfs', *Rev. Mod. Phys.* 65, 301–336 (1993).

21. S. Auddy, S. Basu, and S. R. Valluri, 'Analytic models of brown dwarfs and the substellar mass limit', *Advances in Astronomy* 2016, 5743272 (2016).

22. D. Saumon, W. B. Hubbard, A. Burrows, T. Guillot, J. I. Lunine, and G. Chabrier, 'A theory of extrasolar giant planets', *The Astrophysical Journal* 460, 993 (1996).

23. D. S. Spiegel, A. Burrows, and J. A. Milsom, 'The Deuterium-Burning Mass Limit for Brown Dwarfs and Giant Planets', *The Astrophysical Journal* 727, 57 (2011).

24. K. L. Luhman, V. Joergens, C. Lada, J. Muzerolle, I. Pascucci, and R. White, 'The Formation of Brown Dwarfs: Observations', *arXiv:astro-ph/0608546* (2006).

25. J. Jeans, 'The Stability of a Spherical Nebula', *Philosophical Transactions of the Royal Society of London Series A* 199, 1–53 (1902).

26. M. J. Rees, ‘Opacity-limited hierarchical fragmentation and the masses of protostars’, *Monthly Notices of the Royal Astronomical Society* 176, 483–486 (1976).

27. P.-H. Chavanis, ‘Statistical mechanics of self-gravitating systems in general relativity: I. The quantum Fermi gas’, *Eur. Phys. J. Plus* 135(3), 290 (2019).

28. G. Horedt, ‘*Polytropes - Applications in Astrophysics and Related Fields*’, (Kluwer Academic Publishers, Dordrecht, 2004).

29. S. Chandrasekhar, ‘*An introduction to the study of stellar structure*’, (The University of Chicago press, Chicago, 1939).

30. E. Clapeyron, ‘Mémoire sur la puissance motrice de la chaleur’, *Journal de l'École Polytechnique* XIV, 153–190 (1834).

31. G. Chabrier, D. Saumon, W. B. Hubbard, and J. I. Lunine, ‘The molecular-metallic transition of hydrogen and the structure of Jupiter and Saturn’, *Astrophysical Journal* 391, 817 (1992).

32. H. J. Lane, ‘On the theoretical temperature of the Sun, under the hypothesis of a gaseous mass maintaining its volume by its internal heat, and depending on the laws of gases as known to terrestrial experiment’, *American Journal of Science* 50, 57–74 (1870).

33. A. Ritter, ‘On the Constitution of Gaseous Celestial Bodies’, *Astrophysical Journal* 8, 293 (1898).

34. R. Emden, ‘*Gaskugeln: Anwendungen der mechanischen Wärmetheorie auf kosmologische und meteorologische probleme*’, (B.G. Teubner, Leipzig; Berlin, 1907).

35. C. J. Hansen, S. D. Kawaler, and V. Trimble, ‘*Stellar interiors : physical principles, structure, and evolution*’, (Springer, New York, 2004).

36. A. Einstein, translation by A. Engel, ‘*The Collected Papers of Albert Einstein, Volume 6: The Berlin Years: Writings, 1914-1917*’, (Princeton University Press, New Jersey, 1997).

37. B. P. Abbott and LIGO Scientific Collaboration and Virgo Collaboration, ‘Observation of Gravitational Waves from a Binary Black Hole Merger’, *Phys. Rev. Lett.* 116, 061102 (2016).

38. The LIGO Scientific Collaboration, The Virgo Collaboration, The Fermi Gamma-Ray Burst Monitor, and The INTEGRAL, ‘Gravitational Waves and Gamma-Rays from a Binary Neutron Star Merger: GW170817 and GRB 170817A’, *The Astrophysical Journal* 848, L13 (2017).

39. T. P. Sotiriou and V. Faraoni, '$f(R)$ theories of gravity', *Rev. Mod. Phys.* 82, 451–497 (2010).

40. A. G. Riess, A. V. Filippenko, P. Challis, A. Clocchiatti, A. Diercks, P. M. Garnavich, R. L. Gilliland, C. J. Hogan, S. Jha, R. P. Kirshner, B. Leibundgut, M. M. Phillips, D. Reiss, B. P. Schmidt, R. A. Schommer, R. C. Smith, J. Spyromilio, C. Stubbs, N. B. Suntzeff, and J. Tonry, 'Observational evidence from supernovae for an accelerating universe and a cosmological constant', *The Astronomical Journal* 116, 1009–1038 (1998).

41. A. A. Starobinsky, 'Spectrum of relict gravitational radiation and the early state of the universe', *JETP Lett.* 30, 682–685 (1979).

42. A. H. Guth, 'Inflationary universe: A possible solution to the horizon and flatness problems', *Phys. Rev. D* 23, 347–356 (1981).

43. L. Järv and A. Toporensky, 'Global portraits of nonminimal inflation', *Eur. Phys. J. C* 82, 179 (2022).

44. T. Kobayashi, 'Horndeski theory and beyond: a review', *Reports on Progress in Physics* 82, 086901 (2019).

45. M. Zumalacárregui and J. García-Bellido, 'Transforming gravity: From derivative couplings to matter to second-order scalar-tensor theories beyond the Horndeski Lagrangian', *Phys. Rev. D* 89, 064046 (2014).

46. K. Koyama and J. Sakstein, 'Astrophysical probes of the Vainshtein mechanism: Stars and galaxies', *Physical Review D* 91, 124066 (2015).

47. J. Sakstein, 'Testing gravity using dwarf stars', *Physical Review D* 92, 124045 (2015).

48. L. David and N. Karim, 'Degenerate higher derivative theories beyond Horndeski: evading the Ostrogradski instability', *Journal of Cosmology and Astroparticle Physics* 2016, 034–034 (2016).

49. J. Sakstein and B. Jain, 'Implications of the Neutron Star Merger GW170817 for Cosmological Scalar-Tensor Theories', *Physical Review Letters* 119, 251303 (2017).

50. T. Baker, E. Bellini, P. G. Ferreira, M. Lagos, J. Noller, and I. Sawicki, 'Strong constraints on cosmological gravity from GW170817 and GRB 170817A', *Phys. Rev. Lett.* 119, 251301 (2017).

51. A. Vainshtein, 'To the problem of nonvanishing gravitation mass', *Physics Letters B* 39, 393–394 (1972).

52. J. Gleyzes, D. Langlois, F. Piazza, and F. Vernizzi, 'Exploring gravitational theories beyond Horndeski', *Journal of Cosmology and Astroparticle Physics* 2015, 018–018 (2015).

53. J. Sakstein, 'Hydrogen burning in low mass stars constrains scalar-tensor theories of gravity', *Phys. Rev. Lett.* 115, 201101 (2015).

54. A. Wojnar, 'Polytropic stars in Palatini gravity', *Eur. Phys. J. C* 79, 51 (2019).

Appendix A

Deriving the Lane-Emden equation

Our goal is to derive the equation

$$\frac{1}{\xi^2}\frac{d}{d\xi}\left(\xi^3\frac{d\theta}{d\xi}\right)+\theta^n=0\,. \tag{A.1}$$

In order to to this, let us consider the hydrostatic equilibrium equation and the mass equation

$$\frac{dp(r)}{dr}=-\frac{GM(r)\rho(r)}{c^2r^2}, \qquad M(r)=\int_0^r 4\pi r^2\rho(r)dr\,. \tag{A.2}$$

Also, one can introduce the following dimensionless variables,

$$\rho=\rho_c\theta(\xi)^n \qquad \text{and} \qquad p=p_c\theta(\xi)^{n+1}, \tag{A.3}$$

and

$$r=r_c\xi \qquad \text{with} \qquad r_c^2=\frac{p_c(n+1)}{4\pi G\rho_c^2}\,. \tag{A.4}$$

From (A.2) one gets that

$$\frac{1}{\rho(r)}\frac{dp(r)}{dr}=-\frac{GM(r)}{c^2r^2} \tag{A.5}$$

and

$$\frac{dM(r)}{dr}=4\pi r^2\rho(r). \tag{A.6}$$

Therefore, we can write

$$\frac{d}{dr}\left(\frac{1}{\rho(r)}\frac{dp(r)}{dr}\right)=\frac{GM(r)}{c^2r^3}-\frac{4G\pi\rho(r)}{c^2}=\frac{1}{c^2}\left(-\frac{2}{\rho(r)r}\frac{dp(r)}{dr}-4G\pi\rho(r)\right)\,. \tag{A.7}$$

It is easy to see that we just eliminated mass $M(r)$ from our equation, thus, using natural units, meaning $c = 1$, gives

$$\frac{d}{dr}\left(\frac{r^2}{\rho(r)}\frac{dp(r)}{dr}\right) = -4G\pi r^2\rho(r)\ . \tag{A.8}$$

Introducing the dimensionless variables, knowing that $d\xi = \frac{dr}{r_c}$, allows to write

$$\frac{1}{r^2}\frac{d}{dr}\left(\frac{r^2}{\rho(r)}\frac{dp(r)}{dr}\right) = -4G\pi\rho_c\,\theta(\xi)^n\ , \tag{A.9}$$

where

$$\begin{aligned}\frac{1}{r^2}\frac{d}{dr}\left(\frac{r^2}{\rho(r)}\frac{dp(r)}{dr}\right) &= \frac{1}{r_c^2\xi^2}\frac{d}{r_c d\xi}\left(\frac{r_c^2\xi^2 p_c(n+1)}{\rho_c}\frac{d\theta}{r_c d\xi}\right)\\ &= \frac{p_c(n+1)}{\rho_c r_c^2\xi^2}\frac{d}{d\xi}\left(\xi^2\frac{d\theta}{d\xi}\right)\ .\end{aligned} \tag{A.10}$$

This gives us

$$\frac{p_c(n+1)}{\rho_c r_c^2\xi^2}\frac{d}{d\xi}\left(\xi^2\frac{d\theta}{d\xi}\right) = -4G\pi\rho_c\theta(\xi)^n \tag{A.11}$$

or

$$\frac{p_c(n+1)}{4G\pi\rho_c^2}\frac{4\pi G\rho_c^2}{p_c(n+1)}\cdot\frac{1}{\xi^2}\frac{d}{d\xi}\left(\xi^2\frac{d\theta}{d\xi}\right) = -\theta(\xi)^n\ . \tag{A.12}$$

From this, one gets that

$$\frac{1}{\xi^2}\frac{d}{d\xi}\left(\xi^2\frac{d\theta}{d\xi}\right) = -\theta(\xi)^n\ , \tag{A.13}$$

which is the Lane-Emden equation, that we needed to derive.

There are two boundary conditions for LEE. Firstly, in order to have $\rho(0) = \rho_c$, where ρ_c is defined as the central density, $\theta(0) = 1$ must be satisfied. For the second boundary condition one must investigate what happens when $\xi = 0$. If $\xi = 0$ then $\frac{d\theta}{d\xi}$ must be 0, otherwise the equation would be undefined (division by 0). Hence, the two boundary conditions are

$$\theta(0) = 1 \qquad \text{and} \qquad \left.\frac{d\theta}{d\xi}\right|_{\xi=0} = 0\ . \tag{A.14}$$

The LEE is analytically solvable in only three cases: $n = 0, 1, 5$. Consequently, for realistical physical objects such as stars or brown dwarf with $n = \frac{3}{2}$ a numerical approach is needed.

Appendix B

Python code for solving the modified LEE

```
import numpy as np
import matplotlib.pyplot as plt

# code original source with slight modifications:
#https://www.youtube.com/watch?v=S0yupkDgyJk

'''code for finding solutions to the LEE for different Upsilon values and
then plotting the corresponding graph'''

dxi = 0.00001
U_s = np.linspace(-0.6, 1.4, 11)
N = 10000000

xi_r = []
dtheta_s = []

fig, axis = plt.subplots(figsize = (15,5))

for U in U_s:
    xi = 0.00001
    theta = 1.0
    dtheta = 0.0
    f1 = 0.0
    theta_sol = []
    xi_sol = []
    for i in range(N):
        f1 += -xi**2*theta**1.5*dxi
        dtheta = f1*(1+1.5*U*xi**2*theta**(1.5-1)/4)**(-1)/xi**2-U*xi**3*theta**(1.5)
        *(1+1.5*U*xi**2*theta**(1.5-1)/4)**(-1)/(2*xi**2)
        theta += dxi*f1*(1+1.5*U*xi**2*theta**(1.5-1)/4)**(-1)/xi**2-dxi*U*xi**3
        *theta**(1.5)*(1+1.5*U*xi**2*theta**(1.5-1)/4)**(-1)/(2*xi**2)
        xi += dxi
        theta_sol.append(np.real(theta))
        xi_sol.append(xi)
        if(theta_sol[i] < 0 and theta_sol[i-1] >= 0):
            #print(U, xi)
            xi_r.append(xi)
            dtheta_s.append(dtheta)
```

```
            break
    if round(U,1) == 0.0:
        axis.plot(xi_sol, theta_sol, color = 'black', linewidth = 2, label = 'U=0 (GR)')
    else:
        axis.plot(xi_sol, theta_sol, label = 'U=' + str(round(U,1)))


#give title and axes labels
axis.set_title('Numerical Solutions to the Lame Emden Equation')
axis.set_ylabel('Dimensionless density')
axis.set_xlabel('Dimensionless radius')
#add a legend
axis.legend(loc = "`upper right", ncol=3)
#show
plt.show()
```

Appendix C

Functions for finding the electron degeneracy parameter and luminosity

```
# Function for solving for psi

def func(y, t, M, gamma, U):
    X = 0.75
    Y = 0.25

    b1 = 2
    nu = 1.6
    mu_1 = ((1+0.5*0.51)*X+Y/4)**(-1)
    mu_e = (X + 0.5*Y)**(-1)
    kR = 0.01

    exponential = (np.array(-np.exp(-1/y), dtype='float64'))[0]

    b = -(5/16)*y*np.log(1+np.exp(-1/y))+(15/8)*y**2*(np.pi**2/3
        + polylog(2, exponential))
    a = (2.5*mu_e)/mu_1

    f_1 = 1.0180973287844315*10**(-18)*b1**(20/7)*mu_1*(kR**(-8/7)*mu_e**(-8/3))
    f_2 = gamma**(5/7)*(1-U/4)**(8/7)

    change_to_year = 3.1536e7 # seconds/year

    return sympify(-f_1*change_to_year*f_2*M**(-23/21)*y**(nu*20/7)*(1+b+a*y)**(12/7))
```

```
def luminosity(y, M, gamma, U):
    X = 0.75
    Y = 0.25

    b1 = 2
    nu = 1.6
    mu_1 = ((1+0.5*0.51)*X+Y/4)**(-1)
    mu_e = (X + 0.5*Y)**(-1)
    kR = 0.01

```

```

    exponential = (np.array(-np.exp(-1/y), dtype='float64'))[0]

    b = -(5/16)*y*np.log(1+np.exp(-1/y))+(15/8)*y**2*(np.pi**2/3
        + polylog(2, exponential))
    a = (2.5*mu_e)/mu_1

    change_to_year = 3.1536e7 # seconds/year

    return sympify(0.072233*M**(26/21)*b1**(20/7)*y**(nu*20/7)*(1-U/4)**(8/7)
        /(kR**(8/7)*gamma**(2/7)**(a*y+b+1)**(2/7)))
```

```
'''Finding psi and luminosity for GR (Y = 0 and gamma = 2.36)'''

# here we get the polylogarithmic equation
from mpmath import *
import numpy as np
from scipy.integrate import odeint
from sympy import sympify

y0 = 1

tmin1 = 10**6
tmax1 = 5*10**6

t1 = np.linspace(tmin1, tmax1, 10**3)
t2 = np.linspace(tmax1, 10**10, 10**3)
t = np.append(t1, t2)

masses = [0.01, 0.03, 0.05, 0.08, 0.09]
sol = []

for m in masses:
    sol.append(odeint(func, y0, t, args = (m, 2.36, 0,)))
```

Lihtlitsents lõputöö reprodutseerimiseks ja lõputöö üldsusele kättesaadavaks tegemiseks

Mina, Kärt Soieva,

1. annan Tartu Ülikoolile tasuta loa (lihtlitsentsi) enda loodud teose

   The cooling process of brown dwarfs in Horndeski theory of gravity,

   mille juhendaja on Aneta Wojnar, PhD, reprodutseerimiseks eesmärgiga seda säilitada, sealhulgas lisada digitaalarhiivi DSpace kuni autoriõiguse kehtivuse lõppemiseni.

2. Annan Tartu Ülikoolile loa teha punktis 1 nimetatud teos üldsusele kättesaadavaks Tartu Ülikooli veebikeskkonna, sealhulgas digitaalarhiivi DSpace kaudu Creative Commonsi litsentsiga CC BY NC ND 3.0, mis lubab autorile viidates teost reprodutseerida, levitada ja üldsusele suunata ning keelab luua tuletatud teost ja kasutada teost ärieesmärgil, kuni autoriõiguse kehtivuse lõppemiseni.

3. olen teadlik, et punktis 1 ja 2 nimetatud õigused jäävad alles ka autorile.

4. kinnitan, et lihtlitsentsi andmisega ei rikuta teiste isikute intellektuaalomandi ega isikuandmete kaitse seadusest tulenevaid õigusi.

Kärt Soieva,
Tartu, 27. mai 2022. a.